Article

Not peer-reviewed version

The generation of ROS by exposure to trihalomethanes promotes the IκBα/NF-kB/p65 complex dissociation in human lung fibroblast

Minerva Nájera-Martínez , Jhonatan Avilez-Alvarado , Nataraj S Pagadala , Ricardo Dzul-Caamal , María Lilia Domínguez-López , Jack Tuszynski , Armando Vega-López *

Posted Date: 11 July 2024

doi: 10.20944/preprints202407.0790.v2

Keywords: Antioxidant defenses; Hydrogen peroxide; IPT domain; Fibroblasts; NF-κB nuclear translocation; Superoxide anion

Article

The Generation of ROS by Exposure to Trihalomethanes Promotes the IκBα/NF-kB/p65 Complex Dissociation in Human Lung Fibroblast

Minerva Nájera-Martínez [1], Jhonatan Avilez-Alvarado [2], Nataraj S. Pagadala [3], Ricardo Dzul-Caamal [4], María Lilia Domínguez-López [5], Jack Tuszynski [6] and Armando Vega-López [1]*

[1] Instituto Politécnico Nacional, Escuela Nacional de Ciencias Biológicas, Laboratorio de Toxicología Ambiental. Av. Wilfrido Massieu s/n, Unidad Profesional Zacatenco, Ciudad de México, CP 07738, México
[2] Instituto Politécnico Nacional, Escuela Superior de Ingeniería Mecánica y Eléctrica, Unidad Culhuacán, Laboratorio de Visión Artificial. Av. Santa Ana 1000, San Francisco Culhuacán CTM V, Ciudad de México, CP 04440, México
[3] Cheminger Inc, Edmonton, Alberta, Canadá, T6x1Z8
[4] Instituto EPOMEX, Universidad Autónoma de Campeche, Av. Héroe de Nacozari No. 480, 24070 San Francisco de Campeche, Campeche, México
[5] Instituto Politécnico Nacional, Escuela Nacional de Ciencias Biológicas, Laboratorio de Inmunoquímica I. Prol. Carpio y Plan de Ayala s/n, Casco de Santo Tomás, Ciudad de México, CP 11340, México
[6] Li Ka Shing Applied Virology Institute, Department of Medical Microbiology and Immunology, University of Alberta, Edmonton, AB, Canada
* Correspondence: avegadv@yahoo.com.mx or avegalo@ipn.mx

Abstract: Disinfection by-products to obtain drinking water, such as CH_2Cl_2, $CHCl_3$, and $BrCHCl_2$, elicit cytotoxicity and hyperproliferation in human lung fibroblasts (MRC-5). Enzymes of their biotransformation modulate these damages and can generate toxic metabolites. However, it is unknown that the response to oxidative stress is involved in cellular hyperproliferation modulated by nuclear factor-kappa B (NF-κB). Hence, MRC-5 cells were treated with these compounds to evaluate ROS, lipid peroxidation, phospho-NF-κB/p65 (Ser536) levels, CAT, SOD, and GPx activities. Further, the interactions of halomethanes and ROS with IκBα/NF-κB/p65 complex were analyzed by molecular docking. The correlation among biomarkers showed positive relationships between the prooxidant damage with the antioxidant response, particularly in cells treated with CH_2Cl_2, and $BrCHCl_2$. Furthermore, negative relationships among ROS with levels of NF-κB/p65 in cells treated with CH_2Cl_2, and $CHCl_3$ were detected. The estimated relative free energy of binding using thermodynamic integration with the p65 subunit of NF-κB was -3.3 kcal/mol for BrCHCl2; -3.5 kcal/mol for both $CHCl_3$ and $O_2\bullet$, and -3.6 kcal/mol for H_2O_2. The chloride and bromide are in close contact with the IPT domain residues, particularly in the RHD region involved in DNA binding. Ser281 is located in the same domain, allowing this protein's phosphorylation. Similarly, both ROS are in contact with IPT domain into region RHD and H_2O_2 as side-chain oxygen with Leu280, adjacent to the phosphorylation site of p65. However, a negative correlation among ROS with phospho- NF-κB/p65 suggests ROS's steric hindrance on the C-terminal domain of NF-κB/p65 is involved in antioxidant response.

Keywords: antioxidant defenses; hydrogen peroxide; IPT domain; fibroblasts; NF-κB nuclear translocation; superoxide anion

Introduction

Under certain pathological conditions, the excessive generation of reactive oxygen species (ROS) and the subsequent cellular oxidative stress exerted by these damages are unavoidable unless an

 doi:10.20944/preprints202407.0790.v2

antioxidant system [1,2] counteracts this oxidative damage. If the cell is inefficient in inducing or regulating the antioxidant protective mechanisms, survival or cell death pathways may be activated to arrest or eliminate the damaged tissue [3,4]. This raises essential inquiries about the molecular mechanisms involved in shifting from pro-survival signaling to pro-cell death signaling due to alterations in oxidative balance. To date, no consensus has been reached on the role of ROS in pro-survival signaling and or cell proliferation of human lung fibroblasts; however, some human fibroblasts, such as those of the skin and palmar fascia, have been shown to proliferate at low ROS, concentrations. Even more, when ROS concentrations were inhibited in cell cultures, these cells' proliferation was also diminished [5].

On the other hand, a diversity of oxidants that occurs in the environment induces lesions, leading to pulmonary fibrosis. These oxidants can also activate genes related to cell growth, cell death, and fibroblasts proliferation [6]. For example, after lung tissue damage, the fibroblasts accumulate excessive amounts of collagen, generally accompanied by the hyper-proliferation of these cells for lung repair [7]. The increase in lung collagen and its fibroblasts induction are associated with pulmonary fibrosis development [8]. In addition to direct damage to lung cells and extracellular matrix, oxidants also contribute to developing pulmonary fibrosis - by affecting cytokines and growth factors. In this regard, nuclear factor-kappa B (NF-κB) activation is involved in pulmonary inflammation pathogenesis [9]. The NF-κB/ proto-oncogene c-Rel family (NF-κB/Rel) plays a role in immune responses such as inflammation and immunity, differentiation, cell growth, apoptosis, and tumorigenesis. In mammals, the NF-κB/Rel family comprises at least five family members: RelA, RelB, NF-κB (p105/p50), NF-κB (p100/p52), and c-Rel [10–13]. Previous studies have reported that inhibitor of IkappaB kinase isoform α (IκBα) forms a complex with NF-kβ, in which multiple residues dispersed throughout the protein interface collectively determine its binding affinity. Besides, p65-nuclear localization signaling polypeptide (NLS) is the significant component of the complex that contributes to the binding affinity and specificity of IκBα [14]. NF-κB–activating agents -induce - IκB phosphorylation triggers - the release of NF-κB - into the nucleus and regulate the gene expression on the κB sites [10,15–17]. However, whether ROS can alter the signaling pathways mediated by NF-κB, possibly involved with hyper-proliferation and other processes in human lung fibroblasts, is not known. This response can occur because phosphorylation is critical in activating NF-κB downstream of physical, oxidative, and genotoxic stress responses, among other stimuli [17].

The interest in studying the role of ROS and biomarkers of the oxidative stress response on activation of NF-κB from our previous study showed that HMs induced hyper-proliferation in human lung fibroblasts accompanied by increases in collagen synthesis [8]. These results have suggested that activation of genes involved in cell adhesion, differentiation, and proliferation was mediated by NF-κB [18]. Therefore, the objective of the current study was to find evidence that relates to the generation of oxidative stress during the production of ROS with the activation of NF-κB in human lung fibroblasts (MRC-5, ATCC cell line) when exposed to chlorinated and brominated HMs such as CH_2Cl_2, trichloromethane ($CHCl_3$, TCM) and $BrCHCl_2$.

Materials & Methods

Culture of Human Lung MRC-5 Fibroblasts and Treatments

Human lung MRC-5 fibroblasts were acquired from ATCC. MRC-5 fibroblasts was cultured in Dulbecco's Modified Eagle Medium and harvested according to a previous study [8]. A volume of 100 µL of cell suspension (40,000 cells/mL) was seeded per well in sterile 96-well flat-bottom plates with the culture medium in 5% CO_2 and 37 ºC and allowed to rest for 48 h for cellular adherence and initial growth before treatment was initiated. Before this, growth kinetics using 10,000, 20,000, 30,000, 50,000, and 100,000 cells/mL was performed at 24, 48, and 72 h to optimize growth conditions and reach 50% confluence before exposure (results not shown) [8]. The HMs used in this study were selected based on the frequency of their occurrence and reported concentrations in drinking water [8,19]. $BrCHCl_2$, $CHCl_3$, and CH_2Cl_2 high-performance liquid chromatography grade were added to the culture medium using autoclave-sterilized 70% glycerol as a vehicle to obtain final concentrations of 10^{-4} to 10^{-20} mol (9 treatments) in addition to absolute control (culture medium + 10% fetal bovine

 doi:10.20944/preprints202407.0790.v2

serum "FBS") and solvent control (culture medium + FBS + glycerol). Treated cells were incubated for 48 h, and the culture medium and each HM concentration were replaced at 24 h. Three independent experiments were performed each time, and vehicle concentration was 1% in all cases. After the treatment and detachment of the cells with trypsin/EDTA solution, cells from 12 wells of the same concentration were collected, mixed, and washed in Eppendorf tubes with phosphate-buffered saline (PBS1X) preheated to 37ºC solution. Samples were centrifuged at 3,200 rpm for 10 min, and the pellet was placed in 100 µL of mammalian protein extraction reagent (M-PER™) lysis solution (Thermo Scientific), sonicated during 30 seg adding 900 µL of PBS 1X. Sample homogenates were divided into two portions: one was centrifuged at 9,000 x g and 4° C for 15 min to obtain the S9 fraction. The uncentrifuged portion and the S9 fraction were stored at −80 °C until the biomarker assay (less than two weeks). The S9 fraction was used for ROS quantification and the enzymatic assays; the uncentrifuged fraction was used to evaluate lipid peroxidation.

Evaluation of Biomarkers

Quantification of ROS ($O_2^{\bullet}$ and H_2O_2) and Level of Lipid Peroxidation as Thiobarbituric Acid Reactive Substances (TBARS)

The ROS measurement was performed in previous reports [20] with 20 µL of S9 fraction of the treated and control cells using a final concentration of 7.0 µmol of dihydroethidium and dihydro-fluorescein diacetate. The concentration of H_2O_2 was calculated with a calibration curve from 0 to 7.0 mol. For $O_2\bullet$, a molar extinction coefficient of 4,669 $mol^{-1}cm^{-1}$ was used for its quantification, considering a light path of 0.67 cm in 96-well plates with 200 µL of final volume. The results were expressed as mol ROS/40,000 cells. The lipid peroxidation evaluated as TBARS was assessed in the uncentrifuged fractions of the treated and control cells by Buege and Aust's method [21]. The lipid peroxidation results were expressed as TBARS with a molar extinction coefficient of 156,000 $mol^{-1}cm^{-1}$ as mol of malondialdehyde (MDA)/40,000 cells. Regarding prooxidant forces (ROS) and lipid peroxidation levels, results were shown by cell number because these biomarkers are not related to protein concentration.

Activity of the Antioxidant Defenses (SOD, CAT and GPx)

The activity of the antioxidant defense enzymes was evaluated in the S9 fraction of the treated and control cells. Superoxide dismutase (SOD; EC 1.15.1.1) activity was evaluated by Misra & Fridovich protocol [22] - using a standard curve (3.73–18.65 UI) of SOD from pure bovine erythrocytes. The results were expressed as mmol/min/mg protein. Catalase (CAT; EC 1.11.1.6) was assessed using the Radi et al. test [23] and was estimated using the molar extinction coefficient of H_2O_2 (0.043 $mmol^{-1}cm^{-1}$). The obtained results were shown as mmol/min/mg protein. The activity of glutathione peroxidase (GPx; EC 1.11.1.9) was evaluated according to Lei et al. method [24] using a test coupled with 1.0 UI of glutathione reductase, 0.03 mol of nicotinamide adenine dinucleotide (NADH), 3.5 mmol of glutathione and 40 mmol H_2O_2 followed by a reading at 340 nm. Enzyme activity was calculated using the molar extinction coefficient of NADH (6.22 $mmol^{-1}$ cm^{-1}). The results were expressed as mmol/min/mg protein. All tests were performed in triplicate, and the total protein content was determined at 660 nm using a protein assay kit.

Assay of Phosphorylated NF-κB/p65 Levels

The sandwich ELISA kit, which detects levels of -NF-κB/p65 phosphorylation at serine 536 - was employed. For the assessment, 100 µL of S9 fraction was placed following the manufacturer's instructions.

Molecular Docking Analysis

Docking studies against the NF-βB/p65 were performed using a docking module implemented in MOE2019 (Chemical Computing Group, Montreal, Canada). In silico docking in MOE, the ligand placement method "Alpha PMI" was employed using London dG scoring function and implicit

 doi:10.20944/preprints202407.0790.v2

generalized born solvation model [25]. The binding sites of the NF-βB/p65 subunit (Protein Data Bank ID: 6QHL) were estimated by using the "alpha site finder" implemented in MOE2014. By default, thirty docked conformations were retained as a cutoff. Finally, the affinity scoring function, ΔG [U total in kcal/mol], was employed to rank the candidate poses as the sum of the electrostatic and Van der Waals energies. The "reaction model" dielectric function with a cutoff between 8 and 10Å and the radius of the interaction site of 6Å was used for our docking studies. The protein-ligand complexes were set up for molecular dynamics and equilibration methods using NAMD 2.5 software [26] and CHARMM22 force field for proteins [27], along with the TIP3P model for water [28]. The simulations began with a 10,000-step minimization of the designed side chains and solvent to remove wrong contacts. A cutoff of 12 A° (switching function starting at 10 A°) for van der Waals interactions was assumed. An integration time step of 2 fs was used, permitting a multiple-time stepping algorithm [29,30] to be employed, in which interactions involving covalent bonds were computed every time step. Short-range non-bonded interactions were computed every two-time step, and long-range electrostatic forces were computed every four-time steps. The pair list of the non-bonded interaction was recalculated every 10-time steps with a pair list distance of 13.5 A°. The short-range non-bonded interactions were defined as van der Waals and electrostatics interactions between particles within 12 A°. A smoothing function was employed for the van der Waals interactions at 10A° distance. The backbone atoms were harmonically constrained with a restraining constant of 10.0 kcal/mol A°2, and the systems were heated to 300 K throughout 6 ps at constant volume. The simulations were equilibrated for 2 ns with NPT ensemble (1 atm, 300 K) while the harmonic constraints were gradually turned off. With no harmonic constraints, the simulations ran for 2 ns in the NPT ensemble using Langevin dynamics at a temperature of 300 K with a damping coefficient of g= 5ps-1 [31]. The pressure was maintained at 1 atm using the Langevin piston method with a piston period of 100 fs, a damping time constant of 50 fs, and a piston temperature of 300 K. Nonbonded interactions were smoothly switched off from 10 to 12 A°. The list of nonbonded interactions was truncated at 14 A°. Covalent bonds involving hydrogen were held rigid using the SHAKE algorithm, allowing a 2-fs time step. No periodic boundary conditions were included in the above studies. Atomic coordinates were saved every 1 ps for the trajectory analysis during the last 2 ns of MD simulation. CHARMM22 force field parameters were used in all simulations in this study. Finally, the graph was drawn by taking Root Mean Square Deviation (RMSD) on the X-axis with time (ns) on the Y-axis. The structure with the least RMSD of Ca trace in the trajectory generated was used for further studies. Finally, self-consistent field (SCF) energies are calculated using wavefunction-based methods that construct an initial guess density matrix by atomic orbital basis functions. At each step, the kinetic energy, nuclear attraction, and electron-electron repulsion terms are calculated, and a correction is applied to the density until self-consistency is achieved.

Statistical Analysis

Results regarding solvent controls were compared using a one-way analysis of variance (ANOVA) followed by Dunnett's test. For phospho- NF-κB/p65, one-way ANOVA followed by the Kruskal–Wallis test was used. Relations between biomarkers were assessed by Pearson correlation analysis. Results were considered significant at $p \leq 0.05$.

Results

The Generation of Hydrogen Peroxide (H_2O_2), Superoxide Anion ($O_2^{\bullet}$), and Lipid Peroxidation by Exposure to Halomethanes (CH_2Cl_2, $CHCl_3$, $BrCHCl_2$) in Human Lung Fibroblasts (MRC-5)

The results showed that the HMs understudy could induce ROS in human lung fibroblasts exposed to different concentrations of these toxicants, particularly superoxide anion. $CHCl_3$ induced higher and more significant ROS production in all test concentrations; in contrast, CH_2Cl_2 and $BrCHCl_2$ elicited different concentrations of ROS production -. Only the lower (10^{-20} to 10^{-14} mol; 1.76-1.66-fold-higher) and the three-fold higher concentrations of CH_2Cl_2 significantly augmented the H_2O_2 production in MRC-5 cells ($p \leq 0.05$), among 2.82 to 1.72-fold-higher, respectively. In the case of

 doi:10.20944/preprints202407.0790.v2

BrCHCl2, the superoxide anion levels showed an irregular response; however, at the two-fold higher concentrations of this halomethane, a significant diminution ($p \leq 0.001$) of H_2O_2 below 0.17-fold-lower was noted (**Figure 1A**,**B**).

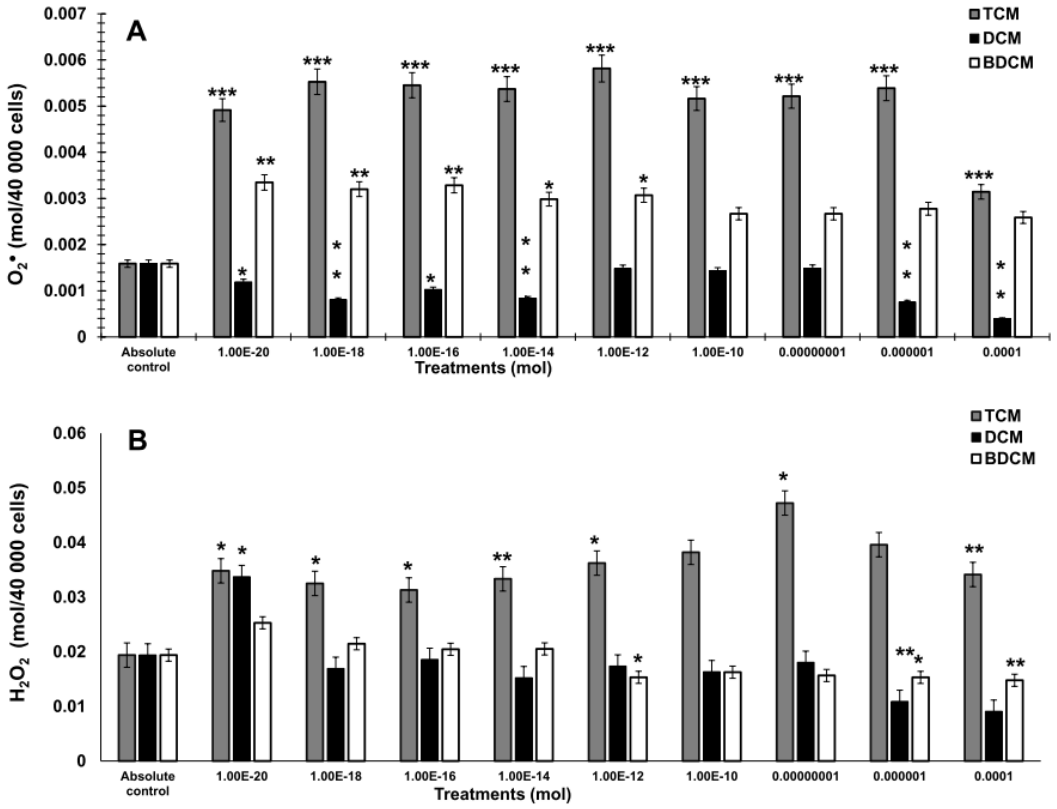

Figure 1. Superoxide anion ($O_2\bullet$) and hydrogen peroxide (H_2O_2) levels on human lung fibroblasts (MRC-5) exposed to dichloromethane (CH_2Cl_2), trichloromethane ($CHCl_3$), and bromodichloromethane ($BrCHCl_2$). **A**) Superoxide anion. **B**) Hydrogen peroxide. Statistical differences regarding absolute control with *$p \leq 0.05$, **$p \leq 0.01$, and ***$p \leq 0.001$. Abbreviations: DCM= CH_2Cl_2; TCM= $CHCl_3$; BDCM= $BrCHCl_2$.

The increase of lipid peroxidation was significantly augmented by exposure to high concentrations of CHCl3 (10-10 to10-6 mol) with increments between 10 to 15.6-fold-higher, and with $BrCHCl_2$ at 10^{-10} mol (1.87- fold-higher). However, higher levels (10^{-8} and 10^{-6} mol) of $BrCHCl_2$ elicited a significant diminution near to 0.12-0.78-fold lower in TBARS. In contrast, an insignificant change of lipid peroxidation was observed in MRC-5 cells exposed to CH_2Cl_2 except for diminishing the oxidative damage close to 0.15-fold-lower in lung fibroblasts exposed to 10^{-6} mol (**Figure 2**).

 doi:10.20944/preprints202407.0790.v2

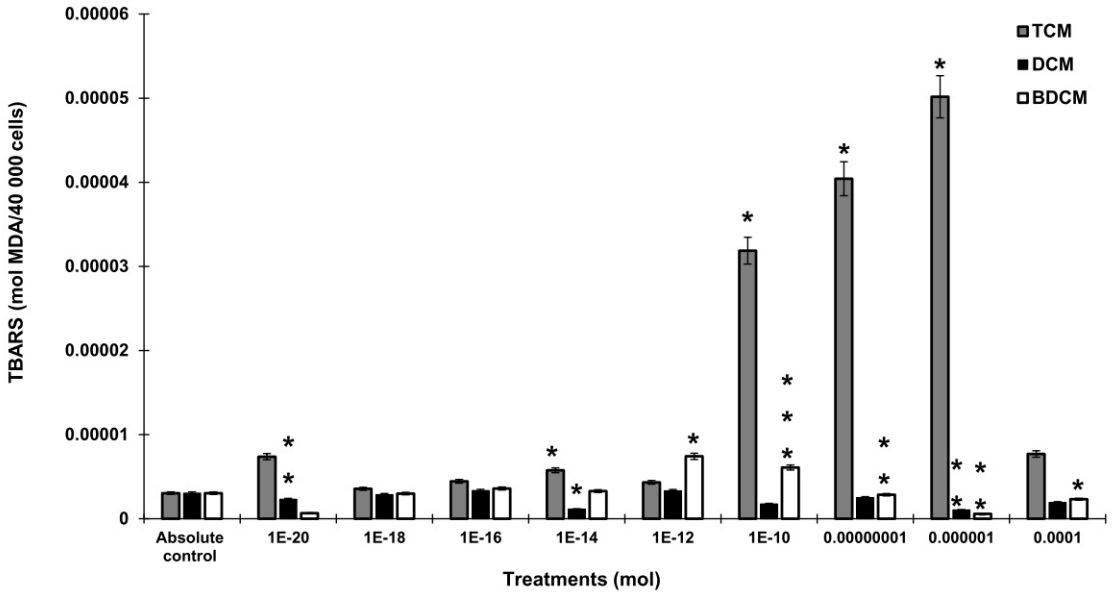

Figure 2. Lipid peroxidation levels evaluated as thiobarbituric acid reactive substances (TBARS) on human lung fibroblasts (MRC-5) exposed to dichloromethane (CH_2Cl_2), trichloromethane ($CHCl_3$), and bromodichloromethane ($BrCHCl_2$). **A**) Superoxide anion. **B**) Hydrogen peroxide. Statistical differences regarding absolute control with *p≤0.05, **p≤0.01, and ***p≤0.001. Abbreviations: DCM= CH_2Cl_2; TCM= $CHCl_3$; BDCM= $BrCHCl_2$.

The Activity of the Antioxidant Enzymes

There were no significant changes in the activity of SOD in the MRC-5 cells exposed to $CHCl_3$. However, the treatments with CH_2Cl_2 and $BrCHCl_2$ irregularly increased this enzyme's catalysis (**Figure 3A**). CAT activity was augmented in all treatments of CH_2Cl_2, particularly at the higher concentrations (3.48-3.51-fold-higher; p≤0.01). In contrast, MRC-5 exposed to $BrCHCl_2$ suffered a significant abolishment in CAT activity at 10^{-12} to 10^{-8} mol (1.83-2.16, fold-higher, p≤0.01); nevertheless, the response of this enzyme could be considered inconsistent in this treatment (**Figure 3B**). The catalysis of GPx was increased in all treatments with $CHCl_3$ and with CH_2Cl_2. However, a concentration-dependent response was not observed. Quite the opposite, $BrCHCl_2$ treatment irregularly improved this enzyme activity on MRC-5 cells (**Figure 3C**).

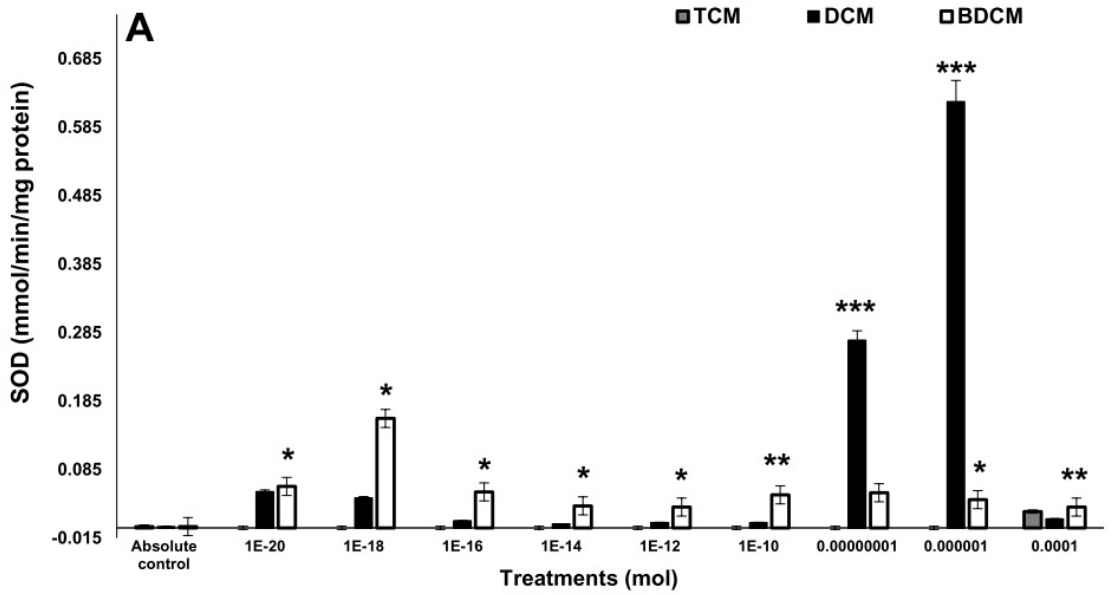

 doi:10.20944/preprints202407.0790.v2

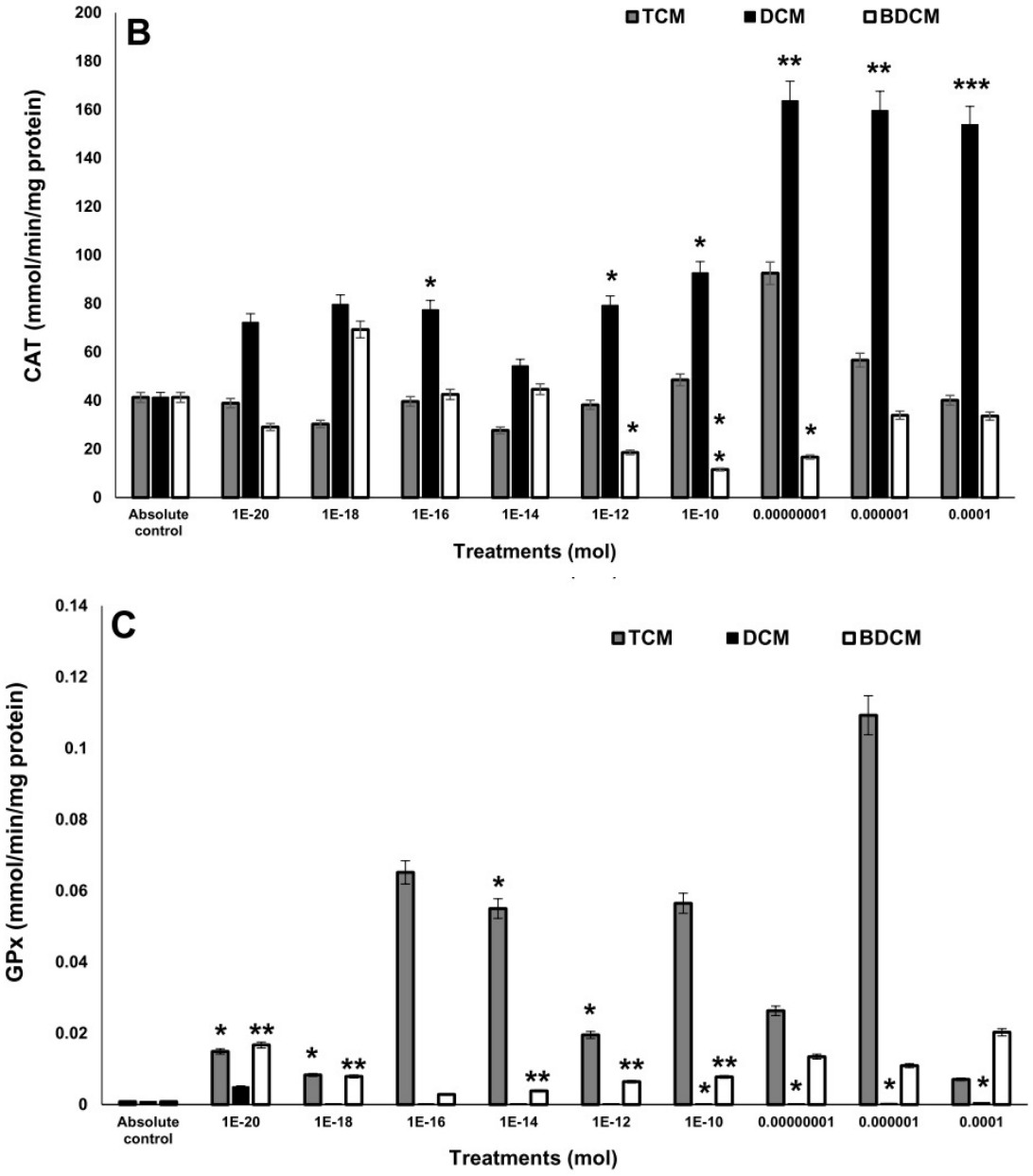

Figure 3. Activity of the enzymes involved in the antioxidant response on human lung fibroblasts (MRC-5) exposed to dichloromethane (CH_2Cl_2), trichloromethane ($CHCl_3$), and bromodichloromethane ($BrCHCl_2$). **A**) Superoxide dismutase. **B**) Catalase. **C)** Glutathione peroxidase. Statistical differences regarding absolute control with *p≤0.05, **p≤0.01, and ***p≤0.001. Abbreviations: DCM= CH_2Cl_2; TCM= $CHCl_3$; BDCM= $BrCHCl_2$.

Evaluation of Phosphorylated NF-κB/p65 Levels

Interestingly, the degree of halogenation of halomethanes seems to be a critical factor in the phosphorylation of NF-κB. Levels of phosphorylated NF-κB at Ser536 on MRC-5 cells exposed to $BrCHCl_2$ increased in a concentration-dependent manner from 10^{-14} to 10^{-6} mol, ranging from 7.15 to 13.5-fold-higher ($p \leq 0.05$). A similar response was observed in MRC-5 cells exposed to $CHCl_3$ from 10^{-12} to 10^{-6} mol, with increments from 1.73 to 3.07-fold higher. However, the phosphorylation of NF-κB induction was lower with $BrCHCl_2$. In contrast, the treatment of CH_2Cl_2 does not induce significant differences regarding control cells (**Figure 4**).

Preprints.org (www.preprints.org) | NOT PEER-REVIEWED | Posted: 11 July 2024 doi:10.20944/preprints202407.0790.v2

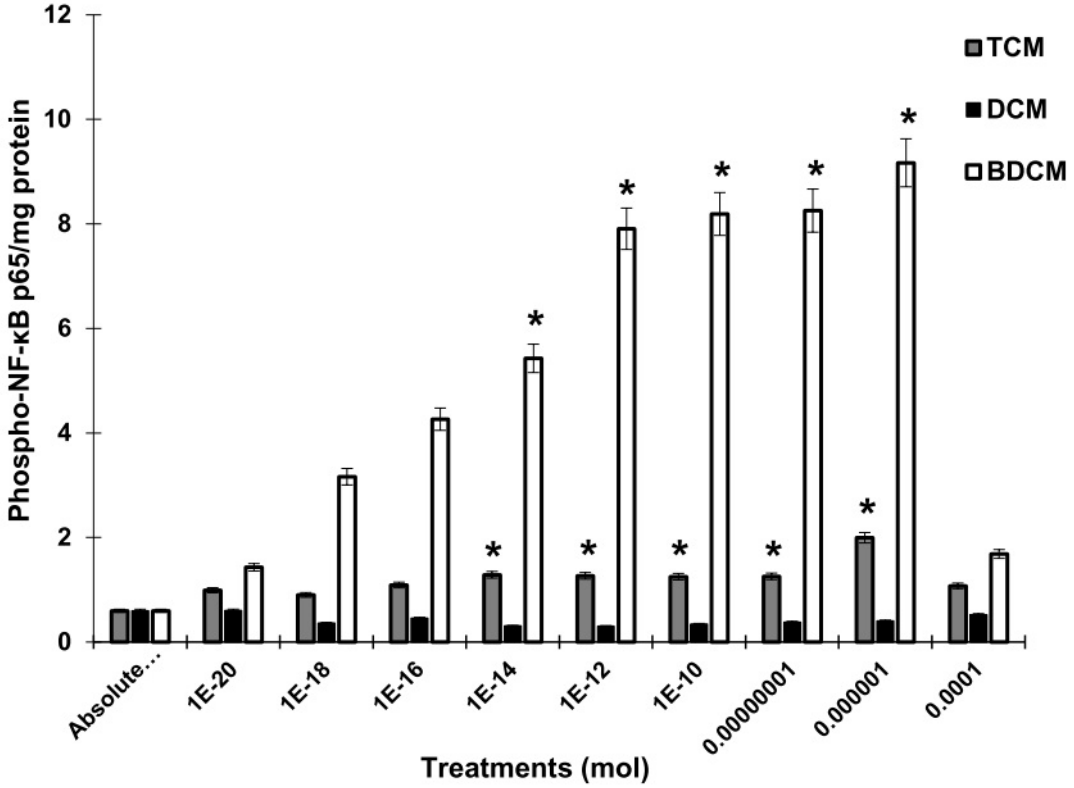

Figure 4. Levels of phosphorylated NF-κB/p65 protein at Ser536 on human lung fibroblasts (MRC-5) exposed to dichloromethane (CH_2Cl_2), trichloromethane ($CHCl_3$), and bromodichloromethane ($BrCHCl_2$). **A**) Superoxide anion. **B**) Hydrogen peroxide. Statistical differences regarding absolute control with *p≤0.05, **p≤0.01, and ***p≤0.001. Abbreviations: DCM= CH_2Cl_2; TCM= $CHCl_3$; BDCM= $BrCHCl_2$.

Relation between Biomarkers

Levels of O_2• were statistically ($p<0.001$) related to H_2O_2 in MRC-5 cells treated with the three HMs under study. The lipid peroxidation was linked with ROS content in this cell line exposed to CH_2Cl_2 and $BrCHCl_2$. In the case of CHCl3, only statistical relationships between TBARS and H_2O_2 were found. The activity of SOD did not show relations with ROS except for $BrCHCl_2$ treatment. In contrast, CAT activity was related to H2O2 on MRC-5 cells exposed to the three HMs, and with O_2• and SOD in the treatments of CH_2Cl_2 and $BrCHCl_2$.

Nevertheless, CAT activity had statistical relationships with TBARS in cells exposed to chlorinated halomethanes. By contrast, GPx showed relations with H_2O_2 in human lung fibroblasts exposed to $BrCHCl_2$ and TBARS in the treatments with $CHCl_3$. Interestingly, both ROS levels were inversely related to phospho- NF-κB/p65 protein at Ser536 on MRC-5 cells exposed to chlorinated halomethanes; besides, O_2• concentration was also linked with this nuclear factor. On the other hand, levels of phospho- NF-κB/p65 protein at Ser536 showed an inverse association with TBARS in the treatment with CH2Cl2 and CAT activity in cells exposed to BrCHCl2 (**Table 1**).

 doi:10.20944/preprints202407.0790.v2

Table 1. Correlation between biomarkers evaluated in human lung fibroblasts (MRC-5) treated with dichloromethane (CH_2Cl_2), trichloromethane ($CHCl_3$), and bromodichloromethane ($BrCHCl_2$) that show the correlation coefficient (R) and the confidence level (*p*). R denotes a pair of biomarkers' direct relationships if this is positive and inverse relationships if this coefficient is negative. Only significant results obtained by the Pearson correlation analysis by each halomethane were shown.

	R, *p*	R, *p*	R, *p*	R, *p*	R, *p*	R, *p*
			CH_2Cl_2			
	H_2O_2	TBARS	SOD	CAT	GPx	NF-κB
O_2•	0.590, <0.001	0.728, <0.001		0.596, <0.001		-0.533, <0.01
H_2O_2		0.736, <0.001		0.541, <0.01		
TBARS				0.408, <0.05		-0.471, <0.01
SOD				0.584, <0.001		
			$CHCl_3$			
	H_2O_2	TBARS	SOD	CAT	GPx	NF-κB
O_2•	0.884, <0.001				0.504, <0.01	-0.611, <0.001
H_2O_2		0.465, <0.05		0.592, <0.001		-0.672, <0.001
TBARS				0.771, <0.001	0.514, <0.01	
			$BrCHCl_2$			
	H_2O_2	TBARS	SOD	CAT	GPx	NF-κB
O_2•	0.915, <0.001	0.418, <0.05	0.539, <0.01	0.682, <0.001	0.407, <0.05	
H_2O_2		0.404, <0.05	0.396, <0.05	0.653, <0.001	0.451, <0.05	
SOD				0.536, <0.01		
CAT						-0.406, <0.05

O_2• Superoxide anion; H_2O_2 Hydrogen peroxide; TBARS lipid peroxidation as thiobarbituric reactive substances; SOD activity of the superoxide dismutase; CAT activity of the catalase; GPx activity of the gluthathione peroxidase; NF-κB levels of the nuclear factor-kappa B.

Molecular Docking Analysis

In this study, the MOE was executed in as much time as required to give several docked conformations. The predicted energy analysis and the consistency of results were considered criteria to identify the best solution for the ligand/receptor model. The *in-silico* results showed that the estimated free energy of binding with the p65 subunit of NF-κB was -7.0 kcal/mol for both $BrCHCl_2$ and H_2O_2: -6.5 kcal/mol for $CHCl_3$, and -7.6 kcal/mol for O_2•. These interaction energy values implied that these ligands could bind with the nuclear factor with sufficient bond strength. In the case of $CHCl_3$, Cl1 bound with Thr191 with a distance of 3.94 Å, Cl2 with Thr191, Ala192, Leu194, and with Ser281 showing distances of 3.37, 2.96, 3.79, and 3.60 Å, respectively. Additionally, Cl_3 was in contact with Leu^{194} at 3.76 Å in region RHD of IPT domain (**Figure 5A**). The Cl_1 anion of $BrCHCl_2$ is - in close contact with – Glu193 and Leu194 and interacts with backbone nitrogen atoms, respectively with the distances of 2.9 and 2.83 Å and electrostatic energy was 0.9 kcal/mol (**Figure 5B**). The Cl_2 and the Br ion contacts with backbone carbon and side chain oxygen of Thr191 with 3.0 Å distances. This finding suggests that backbone nitrogen plays a crucial factor in the interactions of Cl1 and Cl2 with the region RHD of the IPT domain of p65 of NF-κB. The biotransformation of $CHCl_3$ and $BrCHCl_2$ generated ROS (O_2• and H_2O_2), indication both chemical species interact with the NF-κB/p65 complex. Superoxide anion (O_2•) shows only four hydrogen bonds with back bone nitrogens and carbon atoms of Thr191, Ala192, Glu^{193}, Leu^{194} predicting that H_2O_2 shows higher stability than (O_2•) with NF-κB/p65 complex. (**Figure 6A**). However, for H_2O_2, close contacts were detected showing five hydrogen bonds with backbone nitrogens and carbon atoms of Thr^{191}, Ala^{192}, Glu^{193}, Leu^{194}, and side chain oxygen of Leu^{280} (**Figure 6B**). The RMSD of Ca trace on X-axis and time (ns) on Y-axis generated using MD trajectory clearly show that H_2O_2 is highly stable than other ionic species $CHCl_3$, O_2•, and $BrCHCl_2$ showing in order $CHCl_3$<O_2• < $BrCHCl_2$ < H_2O_2 used in this study (**Figure 7A**). In addition, NF-κB/p65- H_2O_2 complex also forms higher number of hydrogen bonds that other three complexes predicting to be high stable (**Figure 7B**). Furthermore, difference in HUMO-LUMO energies calculated for the bound NF-κB/p65-ligand complex also clearly indicated that H_2O_2 and O_2• are chemically stable with -0.3 and -0.5 kcal/mol, respectively, showing a good correlation with ΔG calculated using thermodynamic integration and RMSD stability using MD simulation studies.

 doi:10.20944/preprints202407.0790.v2

However, SCF calculations have shown that $CHCl_3$ shows higher affinity with -46.4 a.u with ΔH of -23.6 kcal/mol, as shown in the **Table 2**.

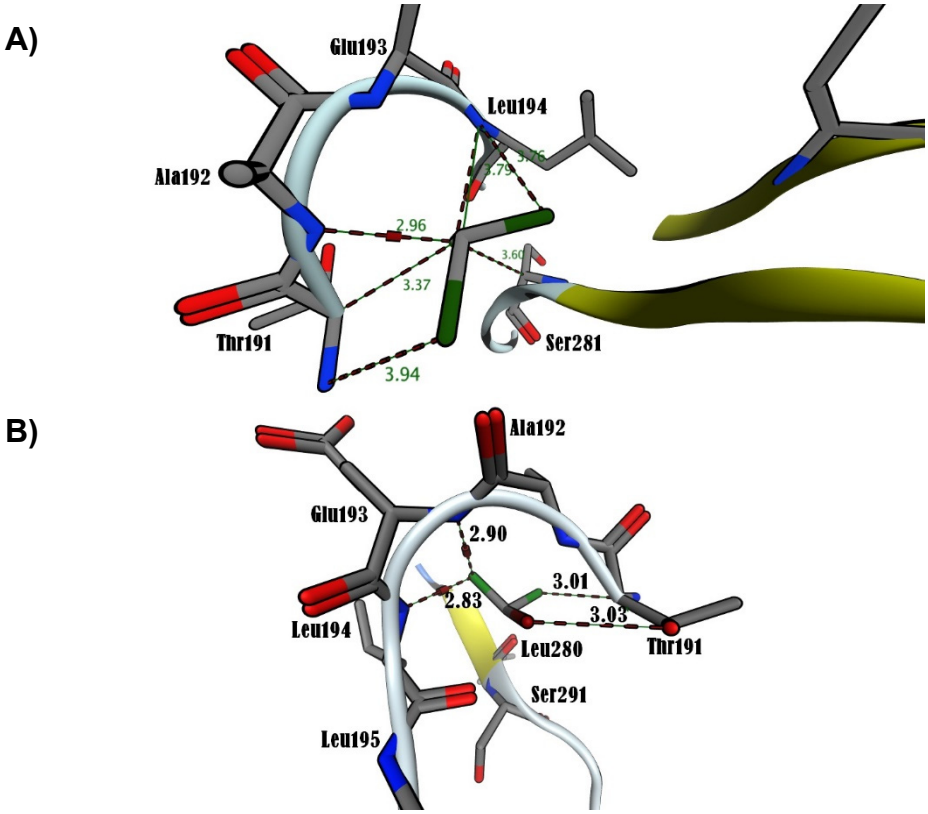

Figure 5. Molecular docking analysis shows the interaction of trihalomethanes with p65 of NF-κB using MOE2019. **A)** Trichloromethane ($CHCl_3$). **B)** Bromodichloromethane ($BrCHCl_2$).

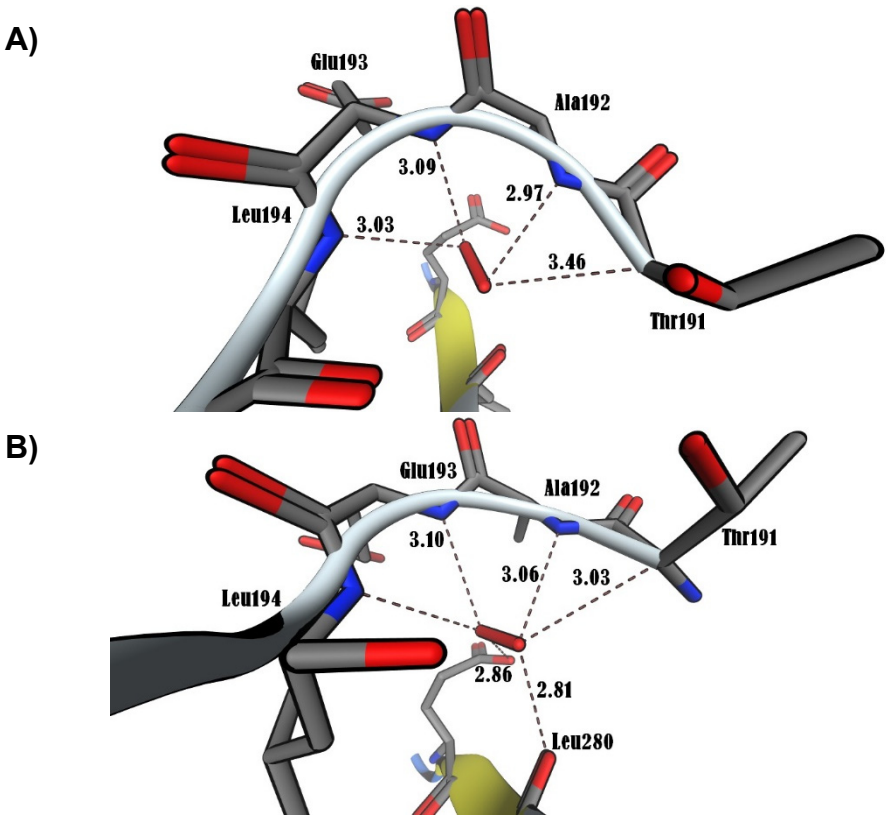

 doi:10.20944/preprints202407.0790.v2

Figure 6. Molecular docking analysis that shows ROS's interaction with p65 of NF-κB using MOE2019. **A)** Superoxide anion (O_2•). **B)** hydrogen peroxide (H_2O_2).

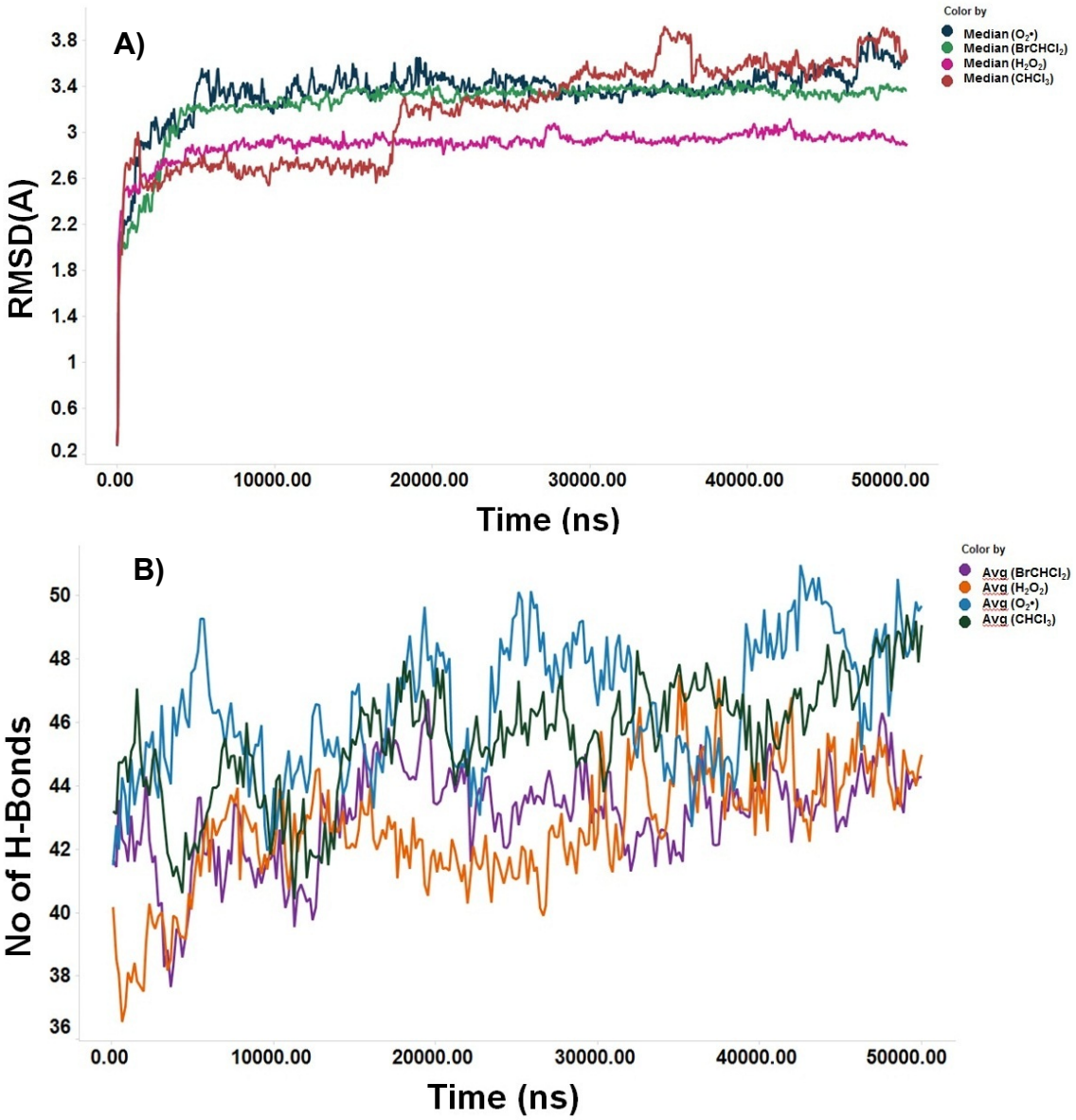

Figure 7. The RMSD of Ca trace on X-axis and time (ns) on Y-axis generated using MD trajectory and number of hydrogen bonds of bromodichloromethane ($BrCHCl_2$), trichloromethane ($CHCl_3$), superoxide anion (O_2•), and hydrogen peroxide (H_2O_2) in contact with NF-κB/p65. **A)** RMSD. **B)** Number of hydrogen bonds.

Table 2. Self-consistent field (SCF) energies of $BrCHCl_2$, $CHCl_3$, H_2O_2, and O_2• with NF-κB/p65 using wavefunction-based methods. The affinity scoring function, ΔG [U total in kcal/mol], was employed to rank the candidate poses as the sum of the electrostatic and Van der Waals energies.

Compound	SCF (au)	ΔH (kcal/mol)	ΔE(eV)	ΔG (kcal/mol)
$CHCl_3$	-46.4	-23.6	11.6	-3.5
$BrCHCl_2$	-23.9	-17.9	12.5	-3.3
O_2•	-24.4	-35.3	0.5	-3.6
H_2O_2	-45	-15.5	0.3	-3.6

 doi:10.20944/preprints202407.0790.v2

Discussion

The lungs are commonly affected by ROS, and almost all cell types of this organ can produce these highly reactive molecules. Under basal conditions, ROS are synthesized by NADPH oxidase and act as second messengers to activate numerous intracellular proteins and enzymes involved in physiological and pathological stages [19,32]. In the lungs, pulmonary fibroblasts produce ROS, especially after stimulation by inflammatory cytokines [33] with a diverse range of stimuli. However, uncontrolled ROS production could directly cause DNA damage, morphologic transformations in cells, and lung injury if the antioxidant system cannot control the generation of ROS [34,35]. Besides, in the environment, many toxicants can induce these prooxidant forces [36,37]. Nevertheless, there is no previous information about ROS production in human lung fibroblasts induced by HMs, a by-product of disinfection procedures to produce drinking water. The current study found that the toxicants understudy could induce ROS *in vitro*, particularly O_2•. Similar findings were also observed in peripheral blood mononuclear cells (PBMCs) of *Cyprinus carpio carpio* i.p dosed with CH_2Cl_2, $CHCl_3$ and $BrCHCl_3$ [19]. Despite this lack of information, we can propose that the generation of ROS in human fibroblasts treated with halomethanes is due to a series of events, not necessarily consecutive, as well as its feedback with prooxidant forces and oxidative damage summarized as follows: *1)* Biotransformation processes are fundamental in the generation of ROS. *2)* ROS generation is not directly regulated by mitochondrial activity. *3)* The higher the number of halogens involved, the greater the probability of ROS generation. *4)* Some physicochemical properties, such as the electronegativity of the metabolites generated during biotransformation, influence the ROS generation rate. *5)* ROS induction depends mainly on specific and non-specific antioxidant defenses. The arguments presented are discussed below. ROS could be generated more by an independent pathway than mitochondrial complex I activity [19], such as the case of decoupling the flow of electrons during redox processes of cytochrome P450 isoenzymes (i.g. cytochrome P450 isoform 2E1 "CYP 2E1"). Other enzymes are involved in the HM's bioactivation process, as in the isoform *tetha* of the glutathione S-transferase (GSTT) [8,19,38–40]. Regarding the topic, the obtained results showed that the degree of chlorination of HMs is a critical factor in the induction of ROS in MRC-5 cells. In the first step of the biotransformation of the HMs, the three compounds under study can induce similar amounts of O_2• mediated by the activity of CYP 2E1 [19]. Next to this step, the HMs possessing three halogens suffer reductions, dehalogenations, and reductive dehalogenation mediated by some enzymes such as GSTT and other enzymes [8,41], allowing ROS generation [19]. However, the higher levels of O_2• elicited by $CHCl_3$ compared with $BrCHCl_2$ could be explained by HCl release, which possesses an electronegativity value (δ=1.06) higher than HBr (δ=0.86) released from $BrCHCl_2$ after dehalogenation processes [19]. Contrary to these halomethanes, the amounts of O_2• were the lowest in the cells treated with CH_2Cl_2. This response could be explained by a lesser number of reductive dehalogenations involved in the biotransformation processes that this compound undergoes [19]. Also, on the final step of biotransformation of $CHCl_3$ mediated by GSTT [42], the release of H^+ after reductive dehalogenation probably enhances the respiratory rate and proton motive force [19], allowing ROS generation by mitochondrial complex I activity as well as by mitochondrial electron transport chain. In contrast, the significant diminution of O_2•levels in MRC-5 fibroblasts exposed to high concentrations of CH_2Cl_2 is feasible to explain by enzymatic dismutation of H_2O_2 through SOD activity as demonstrated in the current study. The activity of SOD plays a crucial role in the antioxidant system in human lungs [6,43,44]. This enzyme plays a vital role in the dismutation of O_2• into H_2O_2 and prevents chain reactions that induce •OH and peroxynitrite radicals (ONOO-). However, the O_2• may further convert into OH• in the presence of metal ions via Fenton and Haber-Weiss reactions [45]. The excessive production of ROS in the lungs can disrupt the oxidant/antioxidant balance, vital in developing pathologies in the airways [46–49]. Besides, excessive ROS levels can alter critical cellular components such as proteins, unsaturated lipids, and DNA by exposure to free radicals, thus compromising cell homeostasis [45,50].

On the other hand, the H_2O_2 generation by dismutation of O_2• could occur spontaneously (non-catalyzed) and too mediated by the activity of SOD [45]. The highest levels of H_2O_2 observed in MRC-5 cells treated with CH_2Cl_2 at 10^{-20} mol were not accompanied by the highest concentration of its

 doi:10.20944/preprints202407.0790.v2

precursor (O_2•), which reinforces the hypothesis about a non-catalyzed dismutation, which probably occurred early in the present study, nor the enzymatic activity of SOD had a role, as has been previously reported [45]. In the current study, the H_2O_2 was related to O_2• levels in MRC-5 fibroblasts exposed to $CHCl_3$ but not with SOD activity. This finding suggests a non-catalyzed dismutation of O_2• to H_2O_2 in the presence of H^+ generated during biotransformation at the late stage [19] as observed - for MRC-5 cells treated with CH_2Cl_2. If H_2O_2 levels remain stable in the intracellular medium and escape to the enzymatic action of either CAT or GPx or some non-enzymatic element of the antioxidant system. This compound can activate signaling pathways that stimulate diverse cellular processes such as cell proliferation, differentiation, migration, or apoptosis [19,51–55]. In contrast, levels of H_2O_2 in MRC-5 fibroblasts treated with CH_2Cl_2 and with $BrCHCl_2$ were statistically related to O_2• concentration and showed a similar response in the low treatment. However, in the fibroblasts exposed to $BrCHCl_2$, the diminution of H_2O_2 was linked with the activity of CAT and GPx. Despite the crucial role of CAT in the dismutation of H_2O_2, the role of GPx in maintaining the redox status of lung cells exposed to $BrCHCl_2$ stands out. This enzyme also removes organic hydroperoxides and participates in glutathione's redox cycle, which is abundant in the alveolar epithelial lining fluid [56]. Regardless of the enzymes involved in the antioxidant defense activity, ROS induction elicited lipid peroxidation *in vitro* in human lung fibroblasts.

In addition to the cytotoxicity elicited by HMs previously reported in MRC-5 cells [8], the current study shows that $CHCl_3$-induced lipid peroxidation evaluated as TBARS on this cell line exposed to higher concentrations of this toxicant. The induction of lipid peroxidation was dependent on halomethane concentrations in MRC-5 cells. Indeed, the damage is induced by the remaining amount of ROS generated and not detoxified through the antioxidant defense, as previously discussed. However, this imbalance between the prooxidant forces (ROS) and antioxidants (SOD, CAT, and GPx) produces a series of radical reactions, including, *1)* the initiation caused by the predominance of pro-oxidant forces, *2)* the propagation of free radicals to reach deep levels of damage and destruction of the lipid bilayer and*3)* formation of polymers between free radicals might occur in the best of cases. The background on the subject is set out below. Lipid peroxidation is an oxidative process that involves the deterioration of the lipid bilayer mediated by hydroxyl radical (•OH) to form carbon-carbon double bonds at the initial stage. - The •OH is considered the most critical oxidizing chemical species in the initiation of this process [57]. However, through chain reactions, other chemical species such as alkyl hydroperoxides (LOOH), alkyl peroxyl radicals (LOO•), and alkoxyl radicals (LO) may also be formed [45]. The level of lipid peroxidation induced by $CHCl_3$ was related to H_2O_2 concentration. This oxidation probably implies damages in lung fibroblast membranes (both in the cell and organelles) that can reach several levels of gravity, such as altering the fluidity of the lipid bilayer on its functionality even on its breaking. The consequences can be diverse, but it is possible to emphasize modifications in hormone receptors and proteins involved in signal transduction pathways [45]. A previous report found that a high concentration of $CHCl_3$ elicited a decrease in cell growth of MRC-5 cells in all concentrations assessed; however, higher concentrations of this toxicant induced cytotoxicity [8]. It is possible to speculate that lipid peroxidation elicited by $CHCl_3$ was directly related to various damages, including diminution of lung fibroblast growth and cytotoxicity; however, the lungs could counteract these damages. In this regard, Kornbrust and Mavis [58] reported that lipid peroxidation is about 25 to 50 times higher in the lungs and heart, which are highly oxygenated tissues, than in the liver, kidneys, testes, and brain. Indeed, in lung cells, lipid peroxidation is a process that occurs regularly, but pulmonary fibroblasts are highly effective in remodeling the cells and repairing the damaged tissues. In this regard, the lung can regenerate new cells efficiently after injury. Lung regeneration comprises progenitor cell activation and cell replacement through the proliferation of intact cells [59–61]. Interestingly, the higher concentration of $CHCl_3$ induced a diminution in TBARS levels in MRC-5 cells about the treatment of 10^{-6} mol, which could be due to GPx activity. However, a significant inverse relationship between TBARS and CAT activity also stands out. This response suggests that oxidative damage was provoked by H_2O_2, whose observed decrease to 10^{-4} for 10^{-6} was consistent with increased CAT activity and a decrease in lipid peroxidation. In contrast, in human lung fibroblasts exposed to

 doi:10.20944/preprints202407.0790.v2

$BrCHCl_2$, only the median concentrations elicited an increase in lipid peroxidation, which was related to levels of ROS. However, higher concentrations of this toxicant cause a significant reduction in this oxidative damage, which could be related to increase GPx activity even though a significant relationship was not found. Considering the lung's capacity to repair damaged cells or regenerate new cells after an oxidative injury elicited by ROS, observing the relationships among other biomarkers involved in regulating the cell cycle case of NF-κB is probably helpful.

Remarkably, only the HMs possessing three halogens ($BrCl_2CH$ and Cl_3CH) were able to increase the levels of phospho-NF-κB/p65 protein at Ser536; however, the magnitude of this induction and relationships with the biomarkers of oxidative stress response was different. Although the quantitative structure-activity relationships (QSARs) would offer some explanations about the differentiated response of NF-κB translocation to the nucleus, the molecular docking tools provide detailed information about the disruption of the IκBα- NF-κB/p65 complex by the effects of HMs treatment.

The *in-silico* results using the software molecular operating environment (MOE) showed that the estimated free energy of binding with the p65 subunit of NF-κB was -7.0 kcal/mol for $BrCHCl_2$ and Cl_3CH binds with -6.5 kcal/mol. The interaction energy values implied that these ligands could bind with the nuclear factor with sufficient bond strength, which coincided with the higher phosphorylation levels of NF-κB/p65 in a concentration-dependent manner, particularly for $BrCHCl_2$. The bonds of chloride and bromide from HM have occurred in the C-terminal domain of p65 of NF-κB/p65; this is a relevant finding because the C-terminal transcription activation domain (TAD) regulates the gene expression, and is highly active [62]. Notably, we found that Cl_1, Cl_2, and Br are in contact with four contiguous amino acid residues (Thr^{191}, Ala^{192}, Glu^{193}, Leu^{194}) into region RHD (Rel homology domain), which is involved in DNA-binding. In this sense, it has been reported that the IPT domain is the dimerization segment of the NF-κB/p65 and related transcription factors [63,64], covering 101 a.a. from Thr^{191} to Asp^{291}. Also, the IPT domain acts as a dominant regulator of diverse stressful conditions, including physical stress, oxidative stress, and exposure to certain chemicals [65–67]. Besides, there are critical conserved residues in this domain: Arg198, Glu211, Leu215, and Cys216 in the dimer interface, which is dominated by hydrophobic interactions close to residues of the bond of Cl_1, Cl_2 and bromide anions [68].

On the other hand, post-translational modifications such as phosphorylation, acetylation, and methylation of transcription factors may affect NF-κB transcriptional activity [69]. Remarkably, the phosphorylation of IκB proteins followed by ubiquitination and degradation by proteasomes releases the NF-κB/p65 homodimer, allowing the bind of p65 with DNA as a homodimer or as heterodimers [70–72]. In this context, there are several phosphorylation sites in the IPT domain close to the binding residues of Cl_1, Cl_2 and bromide anions of the HMs, i.e., residues 254, 276, 281, particularly stands out the contact with Ser^{281}. A previous study on a site-directed mutagenesis screen for potential phosphorylation sites within the p65 RHD identified S205, S276, and S281 essential for p65 transcriptional activity [17,73]. These studies and current results suggest that phosphorylation of the NF-κB subunits profoundly affects the function of NF-κB. Certain phosphorylation events contribute to the selective regulation of NF-κB transcriptional activity in a gene-specific manner [74]. In agreement with our result, the binding of the backbone carbon of $CHCl_3$ with Ser281 may affect the complex IκBα/p65 conformation, allowing the hiper-proliferation of MRC-5 as documented in a previous study [8]. In this regard, it has been reported that the phosphorylation of p65 induces a conformational change, which impacts p65 ubiquitination and stability and protein-protein interactions. However, NF-κB/p65 is a highly dynamic and flexible protein not fixed in a globular and well-ordered shape but can change dynamically after NF-κB activation [75]. We consider that the bond of Cl_1, Cl_2 and bromide of $BrCHCl_2$ and $CHCl_3$ would affect the structure of the p65 homodimer as well as its interaction with IκBα, and the dissociation of the Iκβα-NF-κB complex involved in the activation of target genes transcription. However, to evaluate the effects of these HMs in human fibroblasts, the influence of some of the more reactive metabolites derived from biotransformation processes must be considered, such as in the case of ROS.

 doi:10.20944/preprints202407.0790.v2

Despite the preceding results showing relationships among oxidative stress response, and NF-κB/p65 activation [76–86] there is no previous information about ROS production in human lung fibroblasts induced by HMs. However, in a previous study, ROS was inducted in peripheral blood mononuclear cells (PBMCs) of *Cyprinus carpio carpio* i.p treated with CH_2Cl_2, $CHCl_3$ and $BrCHCl_2$ was documented [19]. Results of the current study showed that the toxicants under study induced ROS in vitro with an estimated free energy of binding with NF-κB/p65 of -7.0 kcal/mol for H_20_2 and -7.6 kcal/mol for $O_2\bullet$. The interactions of these ROS occurred in the IPT domain of NF-κB/p65, suggesting the activation of target genes is involved in the antioxidant response, among others, as shown by Pearson correlation analysis. Certain NF-κB-regulated genes play a major role in regulating the amount of ROS in the cell because ROS have various inhibitory or stimulatory roles in NF-κB signaling. The interactions of ROS with cysteine residues are essential to disturb the NF-κB pathways. For example, hydrogen peroxide inhibits IKK activation by acting on its cysteine residues, eliciting, in this way, inhibitory effects in the catalytic domains of tyrosine phosphatases [87,88].

Biochemical analysis in MRC-5 cells treated with HMs and computational study using MOE2019 showed that $BrCHCl_2$ and $CHCl_3$ induce the phosphorylation of NF-κB/p65 by activating the IPT domain. The consequence of these interactions is probably linked with the hyper-proliferation of these cells, as previously documented [8]. However, the ROS generated during the metabolism of these toxicants disturb the activation of the IPT domain involved in the antioxidant response mediated by NF-κB/p65 as observed by negative relationships among ROS with SOD, CAT, and GPx found in cells treated with $CHCl_3$.

Conclusions

The degree of chlorination of $CHCl_3$ and $BrCHCl_2$ is a critical factor in the induction of ROS on MRC-5 lung human fibroblasts, which could be a counterpart to this damage mainly by CAT and GPx activities. Nevertheless, during the biotransformation of these toxicants, the generation of toxic metabolites such as H_2O_2 and $O_2\bullet$ interacts with the phosphorylation site located on IPT domain of NF-κB/p65 complex. However, the higher binding energy of $BrCHCl_2$ with NF-κB/p65 complex accompanied by the significant levels of phospho- NF-κB/p65 allows us to suggest that this halomethane contributes to the dissociation of the IκBα-NFκB complex as well as the transcription of target genes. In contrast, ROS probably disrupts the transcription of other genes, such as the antioxidant enzymes.

Author contributions: MNM conceived, conducted experiments, and wrote the manuscript; JAA conducted experiments; NSP, RDC, MLDL, JT data curation, formal analysis, validation, and visualization; AVL conceived, funding acquisition, project administration, writing - review & editing.

Funding and Acknowledgements: This study was supported by Instituto Politécnico Nacional SIP code 20240926. J. Avilez-Alvarado is a DSc. student of the Instituto Politécnico Nacional who receives a scholarship from CONACyT. M. Nájera-Martinez, M. L. Domínguez-López & A. Vega-López are fellow of Estímulos al Desempeño en Investigación and Comisión y Fomento de Actividades Académicas (Instituto Politécnico Nacional) and Sistema Nacional de Investigadores (SNI, CONACyT, México).

Institutional Review Board Statement: Not applicable.

Informed Consent Statement: Not applicable.

Data Availability Statement: Data supporting reported results are available under request.

Conflicts of Interest: The authors declare no conflict of interest.

References

1. Snezhkina, A.V., Kudryavtseva, A.V., Kardymon, O.L., Savvateeva, M.V., Melnikova, N.V., Krasnov, G.S., Dmitriev, A.A. (2019). ROS Generation and Antioxidant Defense Systems in Normal and Malignant Cells. Oxid. Med. Cell. Longev. (2019) 6175804 https://doi.org/10.1155/2019/6175804
2. Schieber, M., Chandel, N.S. ROS function in redox signaling and oxidative stress. Curr. Biol. 24(2014), R453-62 https://doi.org/10.1016/j.cub.2014.03.034

3. Fulda, S., Gorman, A. M., Hori, O., Samali, A. Cellular Stress Responses: Cell Survival and Cell Death. International J. Cell Biol. 2010, 214074 https://doi.org/10.1155/2010/214074
4. Reuter, S., Gupta, S.C., Chaturvedi, M.M., Aggarwal, B.B. Oxidative stress, inflammation, and cancer: How are they linked? Free Radic. Biol. Med. 49 (2010), 1603–1616 https://doi.org/10.1016/j.freeradbiomed.2010.09.006
5. Wang, L., Li, H., Yang, S. Role of oxygen free radicals in the proliferation of myofibroblasts induced by AngII. Acta Pharm. Sin. B, 3 (2013), 32-37 https://doi.org/10.1016/j.apsb.2012.12.001
6. Kinnula, V. L., Fattman, C. L., Tan, R. J., Oury, T. D. Oxidative Stress in Pulmonary Fibrosis. Am. J. Respir. Crit. Care Med. 172 (2005), 417–422 https://doi.org/10.1164/rccm.200501-017PP
7. Fukushima, K., Satoh, T., Kida, H., Kumanogoh, A. Revisiting Cell Death Responses in Fibrotic Lung Disease: Crosstalk between Structured and Non-Structured Cells. Diagnostic, 10 (2020), 504 https://doi.org/10.3390/diagnostics10070504
8. Nájera-Martínez, M., García-Latorre, E.A., Reyes-Maldonado, E., Domínguez-López, M.L., Vega-López, A. Halomethane-induced cytotoxicity and cell proliferation in human lung MRC-5 fibroblasts and NL20-TA epithelial cells. Inh. Toxicol. 24 (2012), 762–773 https://doi.org/10.3109/08958378.2012.716871
9. Htwe, S. S., Harrington, H., Knox, A., Rose, F., Aylott, J., Haycock, J.W., Ghaemmaghami, A.M. Investigating NF-κB signaling in lung fibroblasts in 2D and 3D culture systems. "Respir. Res. 16 (2015), 144 https://doi.org/10.1186/s12931-015-0302-7
10. Thompson, J. E., Phillips, R. J., Erdjument-Bromage, H., Tempst, P., Ghosh, S. I. kappa B-beta regulates the persistent response in a biphasic activation of NF-kappa B. Cell. 80 (1995), 573–582 https://doi.org/10.1016/0092-8674(95)90511-1
11. Hayden, M.S., Ghosh, S. Shared principles in NF-kappaB signaling. Cell. 132(2008), 344-362 https://doi.org/10.1016/j.cell.2008.01.020
12. Ghosh, S., Dass, F.P.J. Non-canonical pathway network modelling and ubiquitination site prediction through homology modelling of NF-κB. Gene 581 (2016), 48-56 https://doi.org/10.1016/j.gene.2016.01.025
13. Liu, T., Zhang, L., Joo, D., Sun, S.C. NF-κB signaling in inflammation. Signal Transduct. Target. Ther. 2 (2017a), 17023 https://doi.org/10.1038/sigtrans.2017.23
14. Huxford, T., Mishler, D., Phelps, C. B., Huang, D. B., Sengchanthalangsy, L. L., Reeves, R., Hughes, C. A., Elizabeth A. Komives, E. A., Ghosh, G. Solvent Exposed Non-contacting Amino Acids Play a Critical Role in NF-kB/IkBa Complex Formation. J. Mol. Biol. 324 (2002), 587–597 https://doi.org/10.1016/s0022-2836(02)01149-x
15. Chen, Z. J., Parent, L., Maniatis, T. Site-specific phosphorylation of IκB by a novel ubiquitination-dependent protein kinase activity. Cell. 84 (1996), 853–862 https://doi.org/10.1016/s0092-8674(00)81064-8
16. Whiteside, S.T., Epinat, J. C., Rice, N. R., Israel, A. I kappa B epsilon, a novel member of the I kappa B family, controls RelA and cRel NF-kappa B activity. EMBO J. 16 (1997), 1413–1426. https://doi.org/10.1016/j.apsb.2012.12.001
17. Christian, F., Smith, E., Carmody, R. The Regulation of NF-κB Subunits by Phosphorylation. Cells. 5 (2016), 12. https://doi.org/10.3390/cells5010012
18. Sun, X. F. & Zhang, H. NFKB and NFKBI polymorphisms in relation to susceptibility of tumour and other diseases. Histol. Histopathol. 22 (2007), 1387-98. https://doi.org/10.14670/HH-22.1387
19. Uraga-Tovar, D. I., Domíguez-López, M. L., Madera-Sandoval, R. L., Nájera-Martínez, M., García-Latorre, E., Vega-López, A. (2014). Generation of oxyradicals $O_2^{\bullet}$ and H_2O_2), mitochondrial activity and induction of apoptosis of PBMC of *Cyprinus carpio carpio* treated in vivo with halomethanes and with recombinant HSP60 kDa and with LPS of *Klebsiella pneumoniae*. Immunopharmacol. Immunotoxicol. 36 (2014), 329–340. https://doi.org/10.3109/08923973.2014.947034
20. Dzul-Caamal, R., Salazar-Coria, L., Olivares-Rubio, H.F., Rocha-Gómez, M.A., Girón-Pérez, M.I., Vega-López, A. Oxidative stress response in the skin mucus layer of *Goodea gracilis* (Hubbs and Turner, 1939) exposed to crude oil: A non-invasive approach. Comp. Biochem. Physiol., Part A Mol. Integr. Physiol. 200 (2016), 9-20. https://doi.org/10.1016/j.cbpa.2016.05
21. Buege, J. A., Aust, S. D. Microsomal lipid peroxidation. Methods Enzymol. 52 (1978), 302-310. https://doi.org/10.1016/S0076-6879(78)52032-6
22. Misra, H. P., Fridovich, I. The role of superoxide dismutase anion in the autooxidation of epinephrine and a simple assay for superoxide dismutase. J. Biol. Chem. 247 (1972), 3170-3175. https://doi.org/10.1016/S0021-9258(19)45228-9
23. Radi, R., Turrens, J. F., Chang, L.Y., Bush, K. M., Crapo, J. D., Freeman, B.A. Detection of catalase in rat heart mitochondria. J. Biol. Chem. 266 (1991), 22028-22034. PMID: 1657986.
24. Lei, X. G., Evenson, J. K., Thompson, K. M., Sunde, R. A. Glutathione peroxidase and phospholipid hydroperoxide glutathione peroxidase are differentially regulated in rats by dietary selenium. J. Nutr. 125 (1995), 1438–1446. https://doi.org/10.1093/jn/125.6.1438
25. Mackerell, A.D. Jr., Feig, M., Brooks, C.L. 3rd. Extending the treatment of backbone energetics in protein force fields: limitations of gas-phase quantum mechanics in reproducing protein conformational

distributions in molecular dynamics simulations. J. Comput. Chem. 25(2004), 1400-15. https://doi.org/10.1002/jcc.20065
26. Phillips, J.C., Hardy, D.J., Maia, J.D.C., Stone, J.E., Ribeiro, J.V., Bernardi, R.C., Buch, R., et al. Scalable molecular dynamics on CPU and GPU architectures with NAMD. J. Chem. Phys. 153 (2020), 044130. https://doi.org/10.1063/5.0014475
27. MacKerell, A.D., Bashford, D., Bellott, M., Dunbrack, R.L., Evanseck, J.D., Field, M.J., et al. All-atom empirical potential for molecular modeling and dynamics studies of proteins. J. Phys. Chem. B. 102 (1998), 3586-616. https://doi.org/10.1021/jp973084f
28. Jorgensen, W.L., Chandrasekhar, J., Madura, J.D. Comparison of simple potential functions for simulating liquid water. J. Chem. Phys. 79 (1983), 926-935. https://doi.org/10.1063/1.445869
29. Grubmüller, H., Heller, H., Windemuth, A., Schulten, K. Generalized Verlet Algorithm for Efficient Molecular Dynamics Simulations with Long-range Interactions. Mol. Simul. 6 (1991), 121-142. https://doi.org/10.1080/08927029108022142
30. Schlick, T., Skeel, R.D., Brunger, A.T., Kalé, L.V., Board, J.A., Hermans, J., Schulten, K. Algorithmic challenges in computational molecular biophysics. J. Comput. Phys. 151 (1999), 9–48. https://doi.org/10.1006/jcph.1998.6182
31. Brunger, A.T. X-PLOR Version 3.1, A System for X-ray Crystallography and NMR. Yale University, New Haven, CT, USA, 405 p. ISBN: 9780300054026. 1992.
32. Hsu, C. C., Lien, J. C., Chang, C.W., Chang, C. H., Kuo, S. C., Huang, T. F. Yuwen02f1 suppresses LPS-induced endotoxemia and adjuvant-induced arthritis primarily through blockade of ROS formation, NFkB and MAPK activation. Biochem. Pharmacol. 85(2013), 385-95. https://doi.org/10.1016/j.bcp.2012.11.002
33. Tkaczyk, J., Vízek, M. Oxidative Stress in the Lung Tissue – Sources of Reactive Oxygen Species and Antioxidant Defence. Prague Med. Rep. 108(2007), 105–114. PMID: 18225638.
34. Rimal, B., Greenberg, A. K., Rom, W. N. Basic pathogenetic mechanisms in silicosis: current understanding. Curr. Opin. Pulm. Med. 11(2005), 169-73. https://doi.org/10.1097/01.mcp.0000152998.11335.24
35. Mittal, M., Siddiqui, M.R., Tran, K., Reddy, S.P., Malik, A.B. Reactive oxygen species in inflammation and tissue injury. Antioxid. Redox Signal. 20(2014), 1126-67. https://doi.org/10.1089/ars.2012.5149
36. Becklake, M. R. Occupational exposures: evidence for a causal association with chronic obstructive pulmonary disease. Am. Rev. Respir. Dis. 140 (1989), S85-91. https://doi.org/10.1164/ajrccm/140.3_Pt_2.S85
37. Omland, O., Würtz, E.T., Aasen, T.B., Blanc, P., Brisman, J., Miller, M.R., Pederson, O.F., Schlünssen, V., Sigsgaard, T., Ulrik, C.S., Viskum, S. Occupational chronic obstructive pulmonary disease: a systematic literature review. Scand. J. Work Environ. Health. 40(2011), 19-35. https://doi.org/10.5271/sjweh.3400
38. Melnick, R. L., Kohn, M. C., Dunnick, J.K. Regenerative hyperplasia is not required for liver tumor induction in female B6C3F1 mice exposed to trihalomethanes. Toxicol. Appl. Pharmacol. 148(1998), 137–147. https://doi.org/10.1006/taap.1997.8302
39. Vega-López, A., Carrillo-Morales, C. I., Olivares-Rubio, H.F. Evidence of bioactivation of halomethanes and its relation to oxidative stress response in *Chirostoma riojai*, an endangered fish from a polluted lake in Mexico. Arch. Environ. Cont. Toxicol. 62(2012), 479–493. https://doi.org/10.1007/s00244-011-9708-5
40. Dzul-Caamal, R., Olivares-Rubio, H.F., López-Tapia, P., Vega-López, A. Pro-oxidant and antioxidant response elicited by CH_2Cl_2, $CHCl_3$ and $BrCHCl_2$ in *Goodea gracilis* using non-invasive methods. Comp. Bioch. Physiol. A Mol. Integr. Physiol. 165(2013), 515–527. https://doi.org/10.1016/j.cbpa.2013.03.05
41. Dekant, W., Vamvakas, S. Glutathione-dependent bioactivation of xenobiotics. Xenobiotica. 23(1993), 873-87. https://doi.org/10.3109/00498259309059415
42. Zhang, H., Zhang, J., Zhu, Y. In vitro investigations for the QSAR mechanism of lymphocytes apoptosis induced by substituted aromatic toxicants. Fish Shellfish Immunol. 25(2008), 710–717. https://doi.org/10.1074/jbc.M112.388694
43. Crapo, J. D., Tierney, D. F. Superoxide dismutase and pulmonary oxygen toxicity. Am. J. Physiol. 226(1974), 1401–1407. https://doi.org/10.1152/ajplegacy.1974.226.6.1401
44. Birben, E., Sahiner, E. M., Sackesen, C., Erzurum, S., Kalayci, O. Oxidative Stress and Antioxidant Defense. World Allergy Org. J. 5 (2012), 9–19. https://doi.org/10.1097/WOX. 0b013e3182439613
45. Hermes-Lima, M. Oxygen in biology and biochemistry: role free radicals. Functional Metabolism: Regulation and Adaptation. Edited by Kenneth B. Storey. John Wiley & Sons, Inc. 319-368. 2004. https://doi.org/10.1002/047167558X.ch12
46. Finkel, T., Holbrook, N. J. Oxidants, oxidative stress and the biology of ageing. Nature. 408(2000), 239–247. https://doi.org/10.1038/35041687
47. Klaunig, J. E., Kamendulis, L. M. The role of oxidative stress in carcinogenesis. Ann. Rev. Pharmacol. Toxicol. 44(2004), 239-67. https://doi.org/10.1146/annurev.pharmtox.44.101802.121851
48. Gao, F., Kinnula, L. V., Marjukka Myllärniemi, M., Oury, D.T. Extracellular Superoxide Dismutase in Pulmonary Fibrosis. Antioxid. Redox Signal. 10(2008), 343–354. https://doi.org/10.1089/ars.2007.1908

49. Brand, M.D. Mitochondrial generation of superoxide and hydrogen peroxide as the source of mitochondrial redox signaling. Free Rad. Biol. Med. 100(2016), 14-31. https://doi.org/10.1016/j.freeradbiomed.2016.04.001
50. McCord, J. M., Fridovich, I. Superoxide dismutase. An enzymic function for erythrocuprein (hemocuprein). J. Biol. Chem. 244(1969), 6049–6055.
51. Sauer, H., Rahimi, G., Hescheler, J., Wartenberg, M. Role of reactive oxygen species and phosphatidylinositol 3-kinase in cardiomyocyte differentiation of embryonic stem cells. FEBS Lett. 476(2000), 218–223. https://doi.org/10.1016/s0014-5793(00)01747-6
52. Foreman, J., Demidchik, V., Bothwell, J. H., Mylona, P., Miedema, H., Torres, M. A., Linstead, P., Costa, S., Brownlee, C., Jones, J. D. Reactive oxygen species produced by NADPH oxidase regulate plant cell growth. Nature, 422(2003), 442–446. https://doi.org/10.1038/nature01485
53. Geiszt, M., Leto, T.L. The Nox family of NAD(P)H oxidases: host defense and beyond. J. Biol. Chem. 279(2004), 51715–51718. https://doi.org/10.1074/jbc.R400024200
54. Cai, H. Hydrogen peroxide regulation of endothelial function: origins, mechanisms, and consequences. Cardiovasc. Res. 68(2005), 26–36. https://doi.org/10.1016/j.cardiores.2005.06.021
55. Li, J., Stouffs, M., Serrander, L., Banfi, B., Bettiol, E., Charnay, Y., Steger, K., Krause, K. H., Jaconi, M. E. The NADPH oxidase NOX4 drives cardiac differentiation: role in regulating cardiac transcription factors and MAP kinase activation. Mol. Biol. Cell. 17(2006), 3978– 3988. https://doi.org/10.1091/mbc.E05-06-0532
56. Cantin, A. M., North, S. L., Hubbard, R. C., Crystal, R.G. Normal alveolar epithelial lining fluid contains high levels of glutathione. J. Appl. Physiol. 63(1987), 152–157. https://doi.org/10.1152/jappl.1987.63.1.152
57. Ayala, A., Muñoz, M. F., Argüelles, S. Lipid Peroxidation: Production, Metabolism, and Signaling Mechanisms of Malondialdehyde and 4-Hydroxy-2-Nonenal. Oxidative Medicine and Cellular Longevity. Oxid. Med. Cell. Longev. (2014)360438. https://doi.org/10.1155/2014/3604398
58. Kornbrust, D. J., Mavis, R. D. Relative susceptibility of microsomes from lung, heart, liver, kidney, brain and testes to lipid peroxidation: correlation with vitamin E content. Lipids. 15(1980), 315-22. https://doi.org/10.1007/bf02533546
59. Cardoso, W. V., Lu, J. Regulation of early lung morphogenesis: questions, facts and controversies. Development. 133(2006), 1611–1624. https://doi.org/10.1242/dev.02310
60. Cardoso, W. V., Whitsett, J. A. Resident cellular components of the lung: developmental aspects. Proc. Am. Thorac. Soc. 5(2008), 767–771. https://doi.org/10.1513/pats.200803-026HR
61. Morrisey, E. E., Hogan, B. L. Preparing for the first breath: genetic and cellular mechanisms in lung development. Dev. Cell. 18(2010), 8–23. https://doi.org/10.1016/j.devcel.2009.12.010
62. O'shea, J. M., Perkins, N. D. Regulation of the RelA (p65) transactivation domain. Biochem. Soc. Trans. 36(2008), 603–608. https://doi.org/10.1042/bst0360603
63. Cramer, P., Müller, C.W. A firm hand on NFkappaB: structures of the IkappaBalpha-NFkappaB complex. Structure, 7(1999), R1-6. https://doi.org/10.1016/s0969-2126(99)80002-1
64. Li, X., Stark, G.R. NFkappaB-dependent signaling pathways. Exp. Hematol. 30(2002), 285-96. https://doi.org/10.1016/s0301-472x(02)00777-4
65. Zhou, Z., Wang, M., Zhao, J., Wang, L., Gao, Y., Zhang, H., Liu, R., Song, L. increased transcriptional response and translocation of a Rel/NF-κB homologue in scallop *Chlamys farreri* during the immune stimulation. Fish Shellfish Immunol. 34(2013), 1209-15. https://doi.org/10.1016/j.fsi.2013.01.009
66. Du, R.H., Tan, J., Yan, N., Wang, L., Qiao, C., Ding, J.H., Lu, M., Hu, G. Kir6.2 knockout aggravates lipopolysaccharide-induced mouse liver injury via enhancing NLRP3 inflammasome activation. J. Gastroenterol. 49(2014), 727-36. https://doi.org/10.1007/s00535-013-0823-0
67. He, J.Y., Li, P.H., Huang, X., Sun, Y.H., He, X.P., Huang, W., Yu, Z.H. & Sun, H.Y.. Molecular cloning, expression and functional analysis of NF-kB1 p105 from sea cucumber *Holothuria leucospilota*. Dev. Comp. Immunol. 114(2021), 103801. https://doi.org/10.1016/j.dci.2020.103801
68. Huang, D-B., Huxford, T., Chen, Y-Q., Ghosh, G. The role of DNA in the mechanism of NFkB dimer formation: crystal structures of the dimerization domains of the p50 and p65 subunits. Structure. 5(1997), 1427–1436. https://doi.org/10.1016/S0969-2126(97)00293-1
69. Vermeulen, L., De Wilde, G., Notebaert, S., Vanden Berghe, W., Haegeman, G. Regulation of the transcriptional activity of the nuclear factor-κB p65 subunit. Bioch. Pharmacol. 64(2002), 963–970. https://doi.org/10.1016/s0006-2952(02)01161-9
70. Jacobs, M. D., Harrison, S. C. Structure of an IkBa/NF-kB Complex. Cell. 95(1998), 749–758. https://doi.org/10.1016/S0092-8674(00)81698-0
71. Wu, C., Ghosh, S. Differential phosphorylation of the signal-responsive domain of I kappa B alpha and I kappa B beta by I kappa B kinases. J. Biol. Chem. 278(2003), 31980-7. https://doi.org/10.1074/jbc.M304278200
72. Kanarek, N., Ben-Neriah, Y. Regulation of NF-κB by ubiquitination and degradation of the IκBs. Immunol. Rev. 246(2012), 77-94. https://doi.org/10.1111/j.1600-065X.2012.01098-x

 doi:10.20944/preprints202407.0790.v2

73. Anrather, J., Racchumi, G. Iadecola, C. cis-Acting Element-specific Transcriptional Activity of Differentially Phosphorylated Nuclear Factor-κB. J. Biol. Chem. 280(2004), 244–252. https://doi.org/10.1074/jbc.m409344200
74. Cramer, P., Larson, C.J., Verdine, G.L., Müller, C.W. Structure of the human NF-kappaB p52 homodimer-DNA complex at 2.1 A resolution. EMBO J. 16(1997), 7078-90. https://doi.org/10.1093/emboj/16.23.7078
75. Milanovic, M., Kracht, M., Schmitz, M. L. The cytokine-induced conformational switch of nuclear factor κB p65 is mediated by p65 phosphorylation. Bioch. J. 457(2014), 401–413. https://doi.org/10.1042/bj20130780
76. Schwartz, J.L., Antoniades, D.Z., Zhao, S. Molecular and biochemical reprogramming of oncogenesis through the activity of prooxidants and antioxidants. Ann. N. Y. Acad. Sci. 28(1993), 686:262-78, discussion 278-9. https://doi.org/10.1111/j.1749-6632.1993.tb39185.x
77. Dominici, S., Visvikis, A., Pieri, L., Paolicchi, A., Valentini, M.A., Comporti, M. & Pompella, A. Redox modulation of NF-kappaB nuclear translocation and DNA binding in metastatic melanoma. The role of endogenous and gamma-glutamyl transferase-dependent oxidative stress. Tumori. 89(2003), 426-33. PMID: 14606649.
78. Yao, H., Yang, S.R., Kode, A., Rajendrasozhan, S., Caito, S., Adenuga, D., Henry, R., Edirisinghe, I., Rahman, I. Redox regulation of lung inflammation: role of NADPH oxidase and NF-kappaB signalling. Biochem. Soc. Trans. 35Pt 5(2007), 1151-5. https://doi.org/10.1042/BST0351151
79. Zhong, Z.M., Bai, L., Chen, J.T. Advanced oxidation protein products inhibit proliferation and differentiation of rat osteoblast-like cells via NF-kappaB pathway. Cell. Physiol. Biochem. 24(2009), 105-14. https://doi.org/10.1159/000227818
80. Ali, F., Sultana, S. Repeated short-term stress synergizes the ROS signalling through up regulation of NFkB and iNOS expression induced due to combined exposure of trichloroethylene and UVB rays. Mol. Cell. Biochem. 360(2012), 133-45. https://doi.org/10.1007/s11010-011-1051-7.
81. Li, Y., Liu, Y.J., Lv, G., Zhang, D.L., Zhang, L., Li, D. Propofol protects against hydrogen peroxide-induced apoptosis in cardiac H9c2 cells is associated with the NF-κB activation and PUMA expression. Eur. Rev. Med. Pharmacol. Sci. 18(2014), 1517-24. PMID: 24899612.
82. Fenga, C., Gangemi, S., Giambò, F., Tsitsimpikou, C., Golokhvast, K., Tsatsakis, A., Costa, C. Low-dose occupational exposure to benzene and signal transduction pathways involved in the regulation of cellular response to oxidative stress. Life Sci. 147(2016), 67-70. https://doi.org/10.1016/j.lfs.2015.12.025
83. Hu, W., Shi, L., Li, M.Y., Zhou, P.H., Qiu, B., Yin, K., Zhang, H.H., Gao, Y., Kang, R., Qin, S.L., Ning, J.Z., Wang, W., Zhang, L.J. Adrenomedullin protects Leydig cells against lipopolysaccharide-induced oxidative stress and inflammatory reaction via MAPK/NF-κB signalling pathways. Sci. Rep. 7(2017), 16479. https://doi.org/10.1038/s41598-017-16008-x
84. Liu, L., Zuo, Z., Lu, S., Liu, A., Liu, X. Naringin attenuates diabetic retinopathy by inhibiting inflammation, oxidative stress and NF-κB activation in vivo and in vitro. Iran. J. Basic Med. Sc. 20(2017b):813-821. https://doi.org/10.22038/IJBMS.2017.9017
85. He J, Zhou D., Yan B. Eriocitrin alleviates oxidative stress and inflammatory response in cerebral ischemia reperfusion rats by regulating phosphorylation levels of Nrf2/NQO-1/HO-1/NF-κB p65 proteins. Annals of Translational Medicine, 8(2020), 757. https://doi.org/10.21037/atm-20-4258
86. Li, Q., Sun, Y., Liu, B., Li, J., Hao, X., Ge, W., Zhang, X., Bao, S., Gong, J., Jiang, Z., Qiu, C., Zhao, L., Zhao, Y., Chen, Y., Yang, X., Ding, Y., Wu, Z. ACT001 modulates the NF-κB/MnSOD/ROS axis by targeting IKKβ to inhibit glioblastoma cell growth. J. Mol. Med. (Berl), 98(2020), 263-277. https://doi.org/10.1007/s00109-019-01839-0
87. Kamata, H., Manabe, T., Oka, S., Kamata, K., Hirata, H. Hydrogen peroxide activates IkappaB kinases through phosphorylation of serine residues in the activation loops. FEBS Lett. 519(2002), 231–237. https://doi.org/10.1016/s0014-5793(02)02712-6
88. Oliveira-Marques, V., Marinho, H.S., Cyrne, L., Antunes, F. Role of hydrogen peroxide in NF-B activation: From inducer to modulator. Antioxid. Redox Signal. 11(2009), 2223–2243. https://doi.org/10.1089/ars.2009.2601